Application of Level 1 Interaction Formulae to Class 4 Sections

A. Rusch[1] and J. Lindner[2]

[1] Spannverbund GmbH, Fuggerstraße 19, D-10777 Berlin, Germany
[2] Technische Universität Berlin, Fachgebiet Stahlbau, Sekr. TIB 1 - B1,
Gustav-Meyer-Allee 25, D-13355 Berlin, Germany

Abstract

Evaluations are carried out to check the validity of Level 1 interaction formulae to class 4 sections. These interaction formulae are now given in Annex A of prEN 1993-1-1 and called method B. Within these evaluations the standard cases of thin-walled I-sections as well as thinwalled hollow sections subjected to compression and uniaxial bending and compression and biaxial bending are taken into account. The results of several tests and ultimate load calculations are compared with the results received by using the interaction formulae. It is shown that the Level 1 interaction formulae of the future EN code are sufficient economical and safe.

Keywords: thin-walled structures; interaction formulae; beam columns, stability; plate buckling; effective widths

Nomenclature

$\overline{\lambda}_K$	=	non-dimensional member slenderness due to flexural buckling
$\overline{\lambda}_{LT}$	=	non-dimensional member slenderness due to lateral torsional buckling
$\overline{\lambda}_P$	=	non-dimensional plate slenderness due to local buckling
χ	=	reduction factor due to buckling

f_y = yield stress

$\sigma_{cr,P}$ = critical stress due to local buckling

N_{cr} = critical axial force due to overall buckling

M_{cr} = critical moment about the y-axis due to lateral torsional buckling

W_i = section modulus for bending about the axis i

A = area of section

b = width of plate

b_f = width of 3-sided supported plate (e.g. for a flange)

h = height of web of the cross-section

t = thickness of plate

1. Introduction

Several members in a structure are subjected to combined action of compression and bending and called beam columns. The stability check of such members has therefore been always of great interest for structural engineers and is therefore also an important issue of any code of practice for steel structures. Looked at from this point of view especially user friendliness and economy play an important part. Technical committee 8 of ECCS dealt intensively with the problem of interaction formulae for the conversion of the precode of Eurocode 3 (ENV 1992-1-1: 1993) to the final code (EN 1993-1-1). Within a three-step design concept of the EN code new Level 1 interaction formulae were developed [1], [2]. In practical applications the choice of the chosen level depends on the complexity of the treated case, the complexity of the design concept and the intended level of accuracy. The intentions of Level 1 consists in relative simple equations, which can be treated by hand-calculations and the use of internal forces which may be calculated by first order theory. Background informations are given in [15].

The Level 1 interaction formulae for beam columns were developed mainly for class 1 and class 2 sections [1], [2], [15] and intensive evaluations took cross sections into account belonging to these classes. But in principle the design concept will be applied to all section classes 1 to 4. The special effects of the different section classes are to be considered by the cross section properties and by different interaction and imperfection factors. In this paper the new Level 1 interaction formulae for doubly symmetrical I-sections or hollow section are evaluated for class 4 sections, where local buckling influences the load carrying capacity.

2. New Level 1 Interaction Formulae

Basis of the following evaluations is the current draft of prEN 1993-1-1 [3]. The new design concept requires a double check for flexural buckling as well as for lateral torsional buckling.

Flexural buckling (members not susceptible to torsional deformations)

y-y :
$$\frac{N}{\chi_y\, A\, f_y} + k_y \frac{C_{m,y}\, M_y + \Delta M_y}{W_y\, f_y} + \alpha_z\, k_z \frac{C_{m,z}\, M_z + \Delta M_z}{W_z\, f_y} \le 1 \qquad (1)$$

z-z
$$\frac{N}{\chi_z\, A\, f_y} + \alpha_y\, k_y \frac{C_{m,y}\, M_y + \Delta M_y}{W_y\, f_y} + k_z \frac{C_{m,z}\, M_z + \Delta M_z}{W_z\, f_y} \le 1 \qquad (2)$$

Lateral torsional buckling (members susceptible to torsional deformations)

y-y :
$$\frac{N}{\chi_y\, A\, f_y} + k_y \frac{C_{m,y}\, M_y + \Delta M_y}{\chi_{LT}\, W_y\, f_y} + \alpha_z\, k_z \frac{C_{m,z}\, M_z + \Delta M_z}{W_z\, f_y} \le 1 \qquad (3)$$

z-z
$$\frac{N}{\chi_z\, A\, f_y} + k_{LT} \frac{M_y + \Delta M_y}{\chi_{LT}\, W_y\, f_y} + k_z \frac{C_{m,z}\, M_z + \Delta M_z}{W_z\, f_y} \le 1 \qquad (4)$$

The cross section properties and the interaction factors α_y and α_z are obtained from Table 1 in dependency on the section class. Eqs. (5) and (6) define the interaction factors k_y, k_z and k_{LT} for classes

3 and 4. The equivalent uniform moment factors C_m may be determined by Eq. (7) for a linear distributed bending moment M, for other moment distributions see [3].

class 3 and 4: $$k_i = 1 + 0.6\,\bar{\lambda}_{k,i}\,\frac{N}{\chi_i\ A\,f_y} \quad \text{but} \quad k_i \le 1 + 0.6\frac{N}{\chi_i\ A\,f_y} \tag{5}$$

where: i = bending axis y or z

class 3 and 4: $$k_{LT} = 1 - \frac{0.05\,\bar{\lambda}_{K,z}}{C_{m,LT} - 0.25}\frac{N}{\chi_z\ A\,f_y}$$ $$\text{but } k_{LT} \ge 1 - \frac{0.05}{C_{m,LT} - 0.25}\frac{N}{\chi_z\ A\,f_y} \tag{6}$$

for linear moment distribution: $$C_m = 0.6 + 0.4\,\frac{M_2}{M_1} \quad \text{but} \quad C_m \ge 0.4 \tag{7}$$

3. Features of class 4 sections

Effects of local plate buckling usually control the load carrying capacity of thin-walled sections, denominated as class 4 sections in [3]. As shown in Table 1, local plate buckling is taken into account by effective cross-section properties. The values A_{eff} and W_{eff} are calculated each for the relevant loading case only. For example, A_{eff} is calculated under the assumption that an axial force N is present only.

The imperfection factors α and the interaction factors k are identical for class 3 and 4, see Table 1 and Eqs. (5) and (6). But for class 4 it needs to be to emphasized that the interaction factors k as well as the non-dimensional member slendernesses $\bar{\lambda}_K$ and $\bar{\lambda}_{LT}$ are calculated in dependency on the effective properties as defined in Eqs (8) and (9); whereas the bifurcation forces N_{cr} and M_{cr} of the beam column are determined with respect to the gross section. In literature this concept is called Q-factor method [4], [5].

$$\bar{\lambda}_{K,i} = \sqrt{\frac{A_{eff}\ f_y}{N_{cr,i}}} \tag{8}$$

where: i = bending axis y or z

$$\bar{\lambda}_{LT} = \sqrt{\frac{W_{eff,y}\ f_y}{M_{cr}}} \tag{9}$$

Eqs. (1) to (4) and Table 1 show an additional moment ΔM that has to be taken into consideration for class 4 sections. The additional moment depends on the shift e_N of the effective centroid under axial forces. No shift occurs of course for double symmetric sections which are dealt with here for members subjected to axial forces only.

5. Consideration of current research results

The effective cross section properties are calculated using the effective width concept. For four-sided supported plates (such as the web of I-sections) the *Winter* formula Eq. (10) is used, for three-sided supported plates (like the flanges of I-sections) the same *Winter* formula or an improved formula Eq. (11) by the authors can be employed [6]. The *Winter* formula Eq. (10) is in accordance with the recent and the future European standard. Eq. (11) leads to greater ultimate loads especially in the range of high non-dimensional plate buckling slendernesses $\bar{\lambda}_P$ (Eq. (12)).

$$\frac{b_{eff}}{b} = \frac{1}{\bar{\lambda}_P}\left(1 - \frac{0,22}{\bar{\lambda}_P}\right) \tag{10}$$

$$\frac{b_{f,eff}}{b_f} = \frac{1}{\bar{\lambda}_P}\left(1 - \frac{0,22}{\bar{\lambda}_P}\right) + 0.05\ \bar{\lambda}_P \tag{11}$$

$$\bar{\lambda}_P = \sqrt{\frac{f_y}{\sigma_{cr,P}}} \tag{12}$$

The bifurcation stress $\sigma_{cr,P}$ for local plate buckling is each time determined for the entire cross section, thus taking into account the elastic restraint between the cross section elements like flange and web. In practice, $\sigma_{cr,P}$ is often calculated in a simplified way for each cross-section element separately under the assumption of pin-ended support conditions. This type of assumption is generally conservative.

For three-sided supported plates (flanges of I-sections, especially if they are subjected to bending about z-axis), the arrangement of the effective area is very important (Fig. 1). Extensive investigations at *Dortmund University* (Germany), especially by *Brune*, have shown that the current rules of prEN 1993-1-3 underestimate the capacity and the stiffness extremely. Therefore the results from *Dortmund* [7], [8] were introduced in our evaluations. The arrangement of the effective areas due to the proposal of *Brune* is shown in Fig. 4.

The reduction factors χ_y, χ_z for overall flexural buckling stability are calculated using the well known European buckling curves. The reduction factor χ_{LT} for lateral torsional buckling is chosen due to chapter 6.3.2.3 of the present version of prEN1993-1-1 [3] and given by Eqs. (13) and (14).

$$\chi_{LT} = \frac{1}{\Phi_{LT} + \sqrt{\Phi_{LT}^2 - 0.75\,\bar{\lambda}_{LT}^2}} \quad \text{but} \quad \leq 1, \quad \leq \frac{1}{\bar{\lambda}_{LT}^2} \qquad (13)$$

where:

$$\Phi_{LT} = \frac{1}{2}\left[1 + \alpha_Q\left(\bar{\lambda}_{LT} - 0.4\right) + 0.75\,\bar{\lambda}_{LT}^2\right] \qquad (14)$$

Table 2 shows imperfection values α. In refs. [5] and [9] the authors suggest a modified Q-factor method, where the imperfection value α is modified to α_Q (Eq. 15). This modification is a direct consequence from the theoretical background of the Q-factor method [4], though the statistically evaluation of several tests show that it is not absolutely necessary to take α_Q into account.

$$\alpha_Q = \frac{\alpha}{\sqrt{\kappa_P}} \tag{15}$$

where: $$\kappa_P = \frac{A_{eff}}{A} \quad \text{for flexural buckling} \tag{16}$$

$$\kappa_{P,LT} = \frac{W_{eff,y}}{W_{el,y}} \quad \text{for lateral torsional buckling} \tag{17}$$

For bending about the z-axis of I-sections, the existence of a plastic capacity was shown, which can be represented by $W_{eff,z,pl}$ instead of $W_{eff,z}$ [4], [10]. This is partly accounted for by the imperfection factor α_z = 0.8 instead of 1.0 as shown in Table 1. The comparison with test results (Fig. 2) show the plastic capacity to be a useful tool to predict the ultimate load of thin-walled I-sections subjected to bending about the z-axis. For the "simple" geometry of an I-section the plastic section modulus $W_{eff,z,pl}$ can easily be described by Eq. (18), if terms of higher order are neglected.

$$W_{eff,z,pl} = \left(0.5 + \frac{0.17}{\bar{\lambda}_P}\right) W_{eff,z} \tag{18}$$

5. Comparison with test results

Several test series and FE-calculations are taken into account to evaluate the Level 1 interaction formulae Eqs. (1) to (4). For each result (from ultimate load calculation or test), the divisor f is calculated by which the ultimate loads (e.g. N + M_y) must be divided to fulfil the proposed interaction formula. Therefore a value of f > 1 indicates the proposal to be on the safe side whereas a result f < 1 indicates a result on the unsafe side.

Different evaluations were carried out:

a) imperfection factor α (Table 2), plate buckling curve Eq. (11) and $W_{eff,z,pl}$

b) imperfection factor α_Q Eq. (15), plate buckling curve Eq. (11) and $W_{eff,z,pl}$

c) imperfection factor α (Table 2), *Winter* plate buckling curve Eq. (10) and $W_{eff,z}$

d) imperfection factor α_Q Eq. (15), *Winter* plate buckling curve Eq. (10) and $W_{eff,z}$

Assumptions a) and b) take into account all effects in such a way that the greatest ultimate loads are reached. All other simplifications are also safe enough, if for these cases sufficient safety can be shown. For hollow sections the assumptions c) und d) are considered only because no three-sided supported plates are present in this case.

The following tables show the results of the evaluations using the symbols a) to d). The results are given in form of the divisor f as explained before :

Table 3 to 5: I-section subjected to N + M_y, [11], [12], [4]

Table 6 and 7: I-section subjected to N + M_z, [13], [4]

Table 8: I-section subjected to N + M_y + M_z, [4]

Table 9: hollow section subjected to N + M_z (weak axis) [14]

Furthermore Fig. 3 shows the results of Table 4 in detail.

6. Conclusions

New Level 1 interaction formulae are proposed for the conversion of Eurocode 3 (ENV 1993-1-1: 1993) to the final code EN 1993-1-1 [3]. For the sake of user friendliness, the structure of the design concept should be the same for all cross section classes. The development of the new formulae was mainly carried out with regard to class 1 and 2 sections. Therefore extensive evaluations of tests and numerical results of class 4 section were carried out. The results show that the proposed Level 1 formulae give also sufficient economical and safe results for double symmetric sections represented by thin-walled I-sections or hollow sections subjected to compression and bending.

References

[1] Greiner, R., Ofner, R.: Validation of Design Rules for Member Stability of European Standards – Proposal for Buckling Rules. In: *Stability and Ductility of Steel Structures*. Pp. 81-88. Edited by Dubinå, D., Iványi, M. Timisoara, Romania: Elsevier, 1999..

[2] Lindner, J., Rusch, A.: New European Design Concepts for Beam Columns subjected to Compression and Bending. *Advances in Structural Engineering* **4** (2001), pp. 29-41.

[3] prEN 1993-1-1 : 2002 : Eurocode 3 : Design of steel structures, Part 1-1 : General rules and rules for buildings (draft 5 June 2002)

[4] Rusch A.: *Tragfähigkeit von beulgefährdeten, normalspannungsbeanspruchten I-Profilen* [*Load Carrying Capacity of Thin-walled I-sections subjected to normal stresses*]. Ph.D.-Thesis, Berlin, 2000.

[5] Rusch, A, Lindner, J.: Shift of Effective Centroid of centrally Loaded thin-walled I-sections. In: *Coupled Instabilities in Metal Structures CIMS ´2000*. Pp. 189-197. Edited by Camotin, D., Dubinå, D., Rondal, J. Lisbon, Portugal: Imperial College Press, 2000.

[6] Lindner, J., Rusch, A.: Influence of Local Buckling of Flanges on the Ultimate Load of I-Sections. In: *Stability and Ductility of Steel Structures*. Edited by Dubinå, D., Iványi, M. Timisoara, Romania: Elsevier, 1999.

[7] Brune, B.: Die dreiseitig gelagerte Platte in der Methode der wirksamen Breiten [The Three-sided Supported Steel Plate in the Method of Effective Widths]. *Stahlbau* **67** (1998), S. 851-863.

[8] Brune, B.: New Effective Widths of Three-sided Supported Steel Plate and the Influence on coupled Instabilities of Members in Bending and Compression. In: *Coupled Instabilities in Metal Structures CIMS ´2000*. Pp. 189-197. Edited by Camotin, D., Dubinå, D., Rondal, J. Lisbon, Portugal: Imperial College Press, 2000.

[9] Rusch, A., Lindner J.: Lateral Torsional Buckling of Thin-Walled I-sections. In: *NSCC 2001 Proceedings*. Pp. 713-720. Edited by Mäkeläinen, P., Kesti, J., Jutila, A., Kaitila, O. Helsinki, Finland, 2001.

[10] Rusch, A., Lindner, J.: Remarks to the Direct Strength Method. *Thin-walled Structures* **39** (2001), pp. 807-820.

[11] Hasham, A.S., Rasmussen, K.J.R.: Member Capacity of Thin-walled I-Sections in Combined Compression and Major Axis Bending. *Report R746*, University of Sydney, Department of Civil Engineering, June 1997.

[12] Hasham, A.S., Rasmussen, K.J.R.: Interaction Curves for Locally Buckled I-Section Beam-Columns. *Report R762*, University of Sydney, Department of Civil Engineering, January 1998.

[13] Chick, C.G., Rasmussen, K.J.R.: Tests of Thin-walled I-Sections in Combined Compression and Minor Axis Bending Part II. *Report No. R717*, University of Sydney, School of Civil and Mining Engineering, October 1995.

[14] Braham, M., Grimault, J.-P., Rondal, L.: Flambement des profils creux á parois minces, cas des profils rectangulaires chargés axialement. *Rapport final relatif a Convention de recherche Cometube / C.C.E. 6210-SA/3/301,* 1981.

[15] Greiner, R, Lindner, J.: Die neuen Regelungen in der Europäischen Norm En 1993-1-1 für Stäbe unter Druck und Biegung. (New regulations in the euopean code EN 1993-1-1 for members subjected to axial forces and bending moments). Stahlbau 72(2003), under preparation.

Figures captions:

Fig. 1: Arrangement of effective width b'_f of three-sided supported plates (outstand elements)

Fig. 2: I-sections subjected to bending about the z-axis: Ultimate load curves of different design concepts in comparison to test results [4]

Fig. 3: Bending and axial compression N + M_y (calculations of [12]) – members susceptible to torsional deformations: Comparison of numerical results with the modified Q-factor-method: evaluation b)

Fig. 4 Effective widths for outstand compression elements loaded by bending and compression of their transverse edges

Table headings:

Table 1: Cross section properties and interaction factors α_i in dependency on section classes

Table 2: Imperfection factors α in dependency on type of cross section and buckling failure mode

Table 3: Bending and axial compression N + M_y (tests of [11]) – I-sections susceptible to torsional deformations: Comparison of experimental results ($N_{u,test}$) with the (modified) Q-factor-method ($N_{u,Q}$)

Table 4: Bending and axial compression N + M_y (FE-calculations of [12]) – I-sections susceptible to torsional deformations: Statistical evaluation of comparison of 54 numerical results ($N_{u,test}$) with the (modified) Q-factor-method ($N_{u,Q}$), see also Fig. 3

Table 5: Bending and axial compression N + M_y (own tests [4]) – I-sections susceptible to torsional deformations: Comparison of experimental results ($N_{u,test}$) with the (modified) Q-factor-method ($N_{u,Q}$)

Table 6: Bending and axial compression N + M_z (tests of [13]) – I-sections susceptible to torsional deformations: Comparison of experimental results ($N_{u,test}$) with the (modified) Q-factor-method ($N_{u,Q}$)

Table 7: Bending and axial compression N + M_z (own tests [4]) – I-sections susceptible to torsional deformations: Comparison of experimental results ($N_{u,test}$) with the (modified) Q-factor-method ($N_{u,Q}$)

Table 8: Bending and axial compression N + M_y + M_z (own tests [4]) – I-sections susceptible to torsional deformations: Comparison of experimental results (($N_{u,test}$) with the (modified) Q-factor-method ($N_{u,Q}$)

Table 9: Bending and axial compression N + M_z (tests of [14]) – hollow sections: Comparison of experimental results ($N_{u,test}$) with the (modified) Q-factor-method ($N_{u,Q}$)

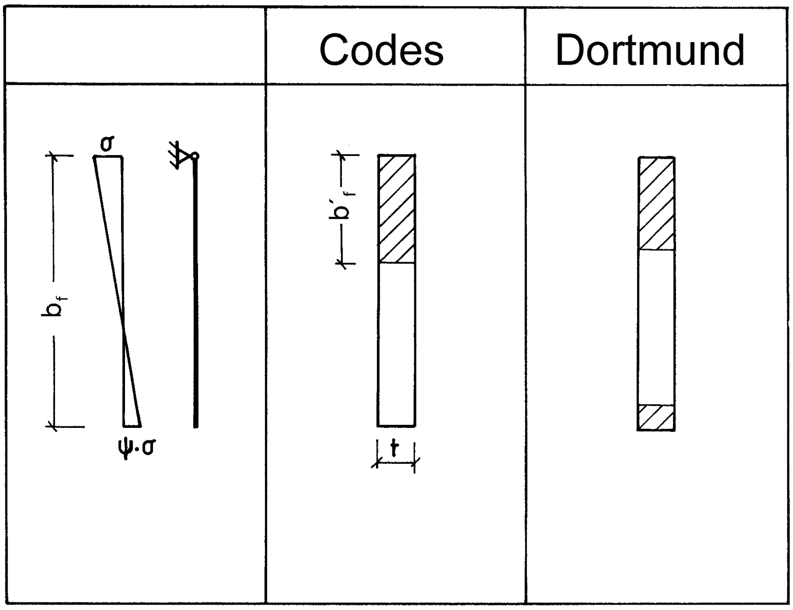

Fig. 1: Arrangement of effective width b'_f for threre-sided supported plates (outstand elements)

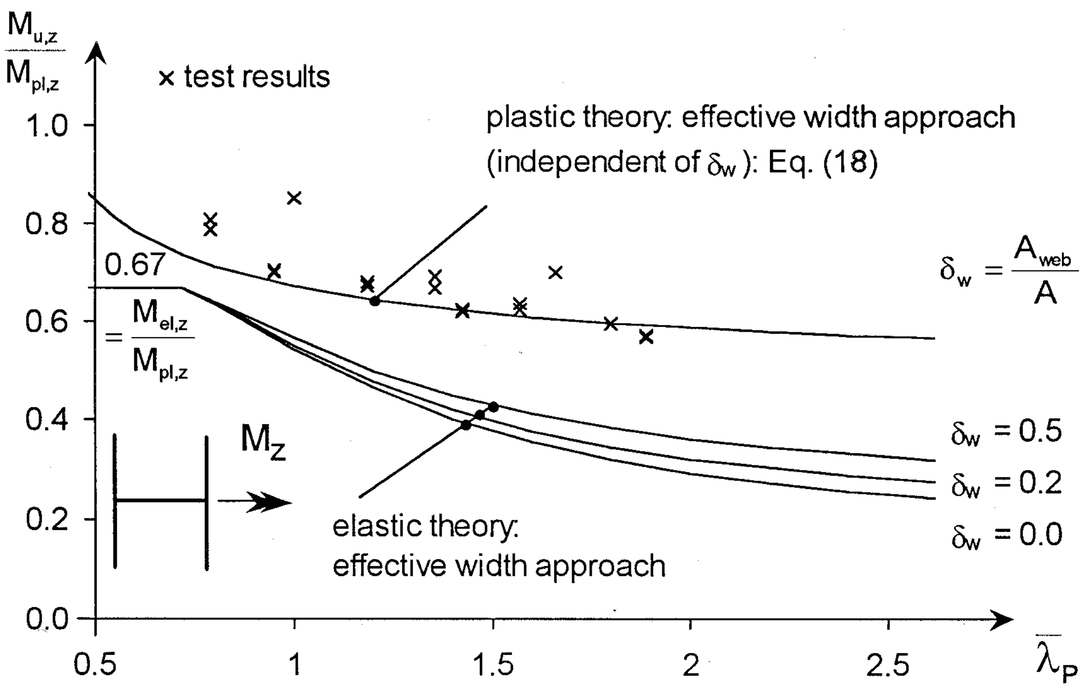

Fig. 2: I-sections subjected to bending about the z-axis: Ultimate load curves of different design concepts in comparison to test results [4]

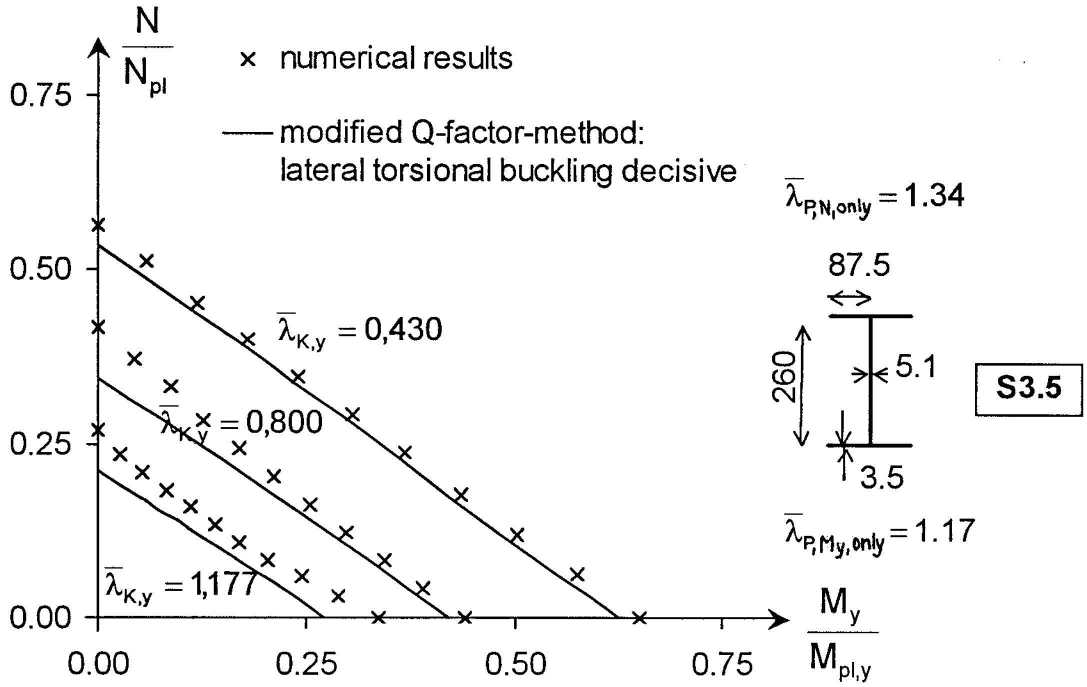

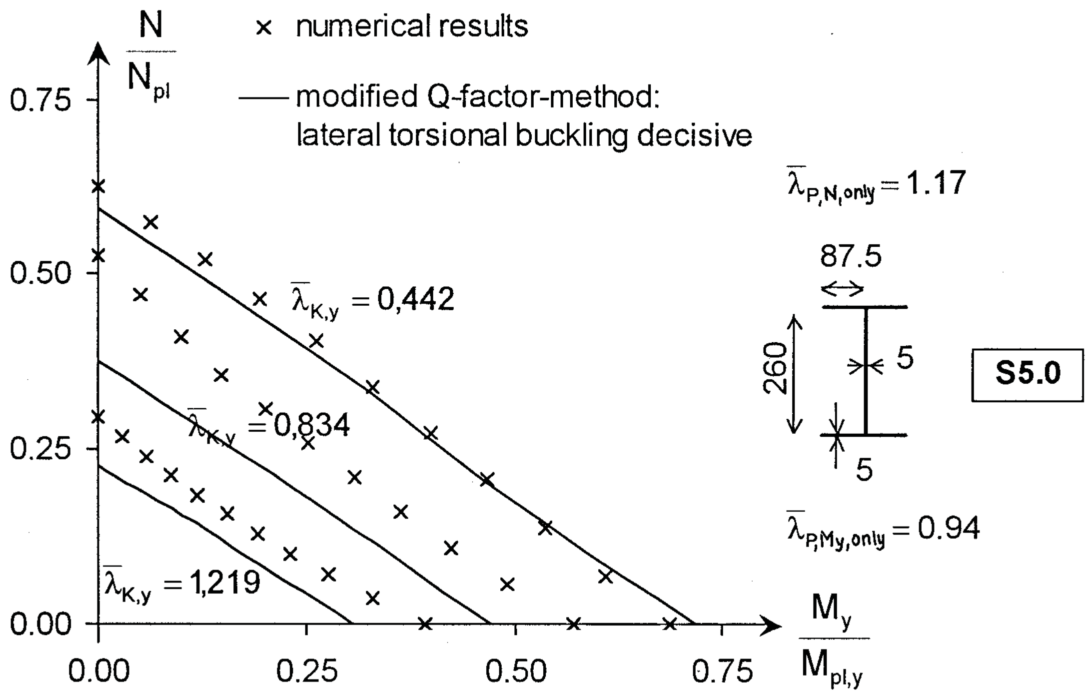

Fig. 3: Bending and axial compression N + M_y (calculations of [12]) – members susceptible to torsional deformations: Comparison of numerical results with the modified *Q-factor*-method: evaluation b)

Fig. 4: Effektive widths for outstand compression elements loaded by bending and compression of their transverse edges

Table 1: Cross section properties and interaction factors α_i in dependency on section class

class	A	W_i	ΔM_i	α_y	α_z
1 and 2	A	$W_{pl,i}$	0	0.6	0.6
3	A	$W_{el,i}$	0	1.0	0.8
4	A_{eff}	$W_{eff,i}$	$e_{N,i}$ N	1.0	0.8
i = bending axis y or z					

Table 2: Imperfection factors α in dependency on cross section

cross section	flexural buckling y-y	flexural buckling z-z	lateral torsional buckling h/b ≤ 2	lateral torsional buckling h/b > 2
welded I-section	curve b $\alpha = 0.34$	curve c $\alpha = 0.49$	curve c_{LT} $\alpha = 0.49$	curve d_{LT} $\alpha = 0.76$
cold-formed hollow section	curve b $\alpha = 0.34$	curve b $\alpha = 0.34$	-	-

Table 3: Bending and axial compression **N + M$_y$** (tests of [11]) – I-sections susceptible to torsional deformations: Comparison of experimental results ($N_{u,test}$) with the (modified) *Q-factor*-method ($N_{u,Q}$):

	b_f	h	t	f_y	plate slenderness	
	[mm]	[mm]	[mm]	[N/mm²]	N: $\bar{\lambda}_{P,N}$	M_y: $\bar{\lambda}_{P,My}$
section:	87,5	260	5	400	0,936	0,632

test	$\bar{\lambda}_{K,y}$	$\bar{\lambda}_{K,z}$	$\bar{\lambda}_{LT}$	$N_{u,test}$	$M_{u,y,test}$	$\frac{N_{u,test}}{N_{u,Q}}$			
	[-]	[-]	[-]	[kN]	[kNm]	a)	b)	c)	d)
SIII0.000	0,310	0,446	0,409	799	0	1,017	1,035	1,062	1,084
SIII0.050				609	25,5	1,030	1,044	1,074	1,090
SIII0.125				421	51,9	1,060	1,068	1,102	1,112
SIII0.250				292	66,5	1,054	1,056	1,094	1,096
SIII0.500				211	80,2	1,094	1,095	1,134	1,135
SIII1.000				0,1	100,0	1,019	1,020	1,053	1,055
SIV0.000	0,563	0,810	0,733	713	0	1,155	1,206	1,200	1,261
SIV0.050				582	25,5	1,257	1,302	1,304	1,359
SIV0.125				397	49,6	1,261	1,297	1,306	1,349
SIV0.250				278	60,9	1,214	1,243	1,256	1,292
SIV0.500				187	70,6	1,195	1,217	1,235	1,263
SIV1.000				0,3	92,2	1,176	1,190	1,213	1,232

Table 4: Bending and axial compression **N + M$_y$** (FE-calculations of [12]) – I-sections susceptible to torsional deformations: Statistical evaluation of comparison of 54 numerical results ($N_{u,test}$) with the (modified) *Q-factor*-method ($N_{u,Q}$), see also Fig. 3

FE	$\frac{N_{u,test}}{N_{u,Q}}$			
	a)	b)	c)	d)
mean value	1,083	1,124	1,117	1,167
standard deviation	0,079	1,091	0,074	0,089

Table 5: Bending and axial compression **N + M$_y$** (own tests [4]) – I-sections susceptible to torsional deformations: Comparison of experimental results ($N_{u,test}$) with the (modified) *Q-factor*-method ($N_{u,Q}$):

test	b_f h_w t	f_y	$\bar{\lambda}_{P,N}$ $\bar{\lambda}_{P,My}$	$\bar{\lambda}_{K,y}$ $\bar{\lambda}_{K,z}$ $\bar{\lambda}_{LT}$	e_z	$N_{u,test}$	$\frac{N_{u,test}}{N_{u,Q}}$			
	[mm]	[N/mm²]	[-]	[-]	[mm]	[kN]	a)	b)	c)	d)
I090	50 200 1,5	161	1,777 1,149	0,137 0,553 0,321	15	42,0	1,061	1,107	1,144	1,199
I004	75 80 1,5	192	1,819 1,719	0,275 0,270 0,159	15	45,1	1,063	1,063	1,215	1,215
I016		174	1,732 1,636	0,310 0,305 0,180	15	39,6	1,013	1,016	1,141	1,145
I132	50 200 2	317	1,868 1,211	0,312 1,264 0,709	50	77,0	1,489	1,643	1,579	1,771
I123	75 80 2	355	1,853 1,754	0,716 0,709 0,401	15	84,6	0,961	1,001	1,092	1,149
I126	50 80 2	336	1,251 1,168	0,719 1,089 0,634	10	76,7	1,213	1,278	1,270	1,353
I136		360	1,208 0,941	0,744 1,127 0,649	41	46,4	1,049	1,099	1,104	1,167

Table 6: Bending and axial compression **N + M$_z$** (tests of [13]) – I-sections susceptible to torsional deformations: Comparison of experimental results ($N_{u,test}$) with the (modified) *Q-factor*-method ($N_{u,Q}$):

	b_f	h	t	f_y	plate slenderness	
	[mm]	[mm]	[mm]	[N/mm²]	N: $\overline{\lambda}_{P,N}$	M_z: $\overline{\lambda}_{P,Mz}$
section:	60	240	5	435	1,424	1,017

test	$\overline{\lambda}_{K,y}$	$\overline{\lambda}_{K,z}$	$\overline{\lambda}_{LT}$	$N_{u,test}$	$M_{u,z,test}$	$\frac{N_{u,test}}{N_{u,Q}}$			
	[-]	[-]	[-]	[kN]	[kNm]	a)	b)	c)	d)
Mz3500-1	0,541	0,730	0,619	799	0	1,249	1,317	1,334	1,418
Mz3500-2				609	25,5	1,165	1,212	1,297	1,356
Mz3500-3				421	51,9	1,185	1,227	1,347	1,399
Mz3500-4				292	66,5	1,094	1,127	1,264	1,305
Mz3500-6				0,1	100,0	1,115	1,121	1,387	1,394
Mz5800-1	0,856	1,154	0,967	713	0	1,116	1,205	1,176	1,288
Mz5800-2				582	25,5	1,039	1,102	1,140	1,221
Mz5800-3				397	49,6	1,088	1,137	1,238	1,301
Mz5800-4				187	70,6	1,071	1,102	1,267	1,307
Mz5800-5				0,3	92,2	1,066	1,066	1,350	1,350

Table 7: Bending and axial compression **N + M$_z$** (own tests [4]) – I-sections susceptible to torsional deformations: Comparison of experimental results ($N_{u,test}$) with the (modified) *Q-factor*-method ($N_{u,Q}$):

test	b_f h_w t	f_y	$\bar{\lambda}_{P,N}$ $\bar{\lambda}_{P,Mz}$	$\bar{\lambda}_{K,z}$	e_y	$N_{u,test}$	$\frac{N_{u,test}}{N_{u,Q}}$			
	[mm]	[N/mm²]	[-]	[-]	[mm]	[kN]	a)	b)	c)	d)
I071	75 40 1,5	154	1,539 1,217	0,271	15	35,9	1,172	1,195	1,424	1,455
I073	75 40 1,9	185	1,334 1,051	0,297	15	56,5	1,151	1,072	1,331	1,358
I018	75 80 1,5	173	1,727 1,302	0,304	30	32,3	1,147	1,150	1,497	1,500
I017		174	1,732 1,306	0,305	30	31,4	1,110	1,113	1,450	1,454
I011		175	1,737 1,310	0,306	15	40,5	1,083	1,088	1,352	1,356
I091	50 200 1,5	161	1,777 0,835	0,553	15	29,9	1,264	1,298	1,405	1,446
I124	75 80 2	317	1,751 1,321	0,670	15	70,3	0,926	0,996	1,143	1,198
I130	75 120 2	326	1,852 1,342	0,714	15	84,2	1,059	1,113	1,306	1,379
I128	50 80 2	355	1,286 0,934	1,119	10	56	1,064	1,114	1,162	1,224

Table 8: Bending and axial compression **N + M_y + M_z** (own tests [4]) – I-sections susceptible to torsional deformations: Comparison of experimental results ($N_{u,test}$) with the (modified) *Q-factor*-method ($N_{u,Q}$)

<table>
<tr><td rowspan="2">test</td><td>b_f
h_w
t</td><td>f_y</td><td>$\bar{\lambda}_{P,N}$
$\bar{\lambda}_{P,My}$
$\bar{\lambda}_{P,Mz}$</td><td>$\bar{\lambda}_{K,y}$
$\bar{\lambda}_{K,z}$
$\bar{\lambda}_{LT}$</td><td>e_z
e_y</td><td>$N_{u,test}$</td><td colspan="4">$\frac{N_{u,test}}{N_{u,Q}}$</td></tr>
<tr><td>[mm]</td><td>[N/mm²]</td><td>[-]</td><td>[-]</td><td>[mm]</td><td>[kN]</td><td>a)</td><td>b)</td><td>c)</td><td>d)</td></tr>
<tr><td>I092</td><td>50
200
1,5</td><td>161</td><td>1,777
1,149
0,835</td><td>0,137
0,553
0,321</td><td>15
15</td><td>30,0</td><td>1,353</td><td>1,386</td><td>1,499</td><td>1,540</td></tr>
<tr><td>I019</td><td rowspan="2">75
80
1,5</td><td>171</td><td>1,717
1,622
1,295</td><td>0,307
0,302
0,179</td><td rowspan="2">1
1</td><td>55,0</td><td>1,060</td><td>1,066</td><td>1,206</td><td>1,210</td></tr>
<tr><td>I014</td><td>175</td><td>1,737
1,641
1,310</td><td>0,311
0,306
0,180</td><td>51,1</td><td>0,971</td><td>0,977</td><td>1,106</td><td>1,111</td></tr>
<tr><td>I067</td><td>50
80
1,5</td><td>222</td><td>1,360
1,268
0,985</td><td>0,361
0,543
0,316</td><td>15
15</td><td>30,6</td><td>1,243</td><td>1,263</td><td>1,411</td><td>1,435</td></tr>
<tr><td>I135</td><td>50
80
2</td><td>318</td><td>1,217
1,136
0,884</td><td>0,699
1,059
0,621</td><td>10
10</td><td>51,4</td><td>1,141</td><td>1,184</td><td>1,232</td><td>1,286</td></tr>
</table>

Table 9: Bending and axial compression **N + M_z** (tests of [14]) – **hollow sections**: Comparison of experimental results ($N_{u,test}$) with the (modified) *Q-factor*-method ($N_{u,Q}$):

	b	h	t	f_y	plate slenderness	
	[mm]	[mm]	[mm]	[N/mm²]	N: $\overline{\lambda}_{P,N}$	M_z: $\overline{\lambda}_{P,Mz}$
section:	150,5	250,5	4,85	388	1,021	0,975
test	$\overline{\lambda}_{K,z}$	$e_{y,top}$	$e_{y,bottom}$	$N_{u,test}$	$\frac{N_{u,test}}{N_{u,Q}}$	
	[-]	[mm]	[mm]	[kN]	c)	d)
R—50EX2-1	0.692	62.8	-62.8	615	0.967	0.982
R—50EX1-1	0.692	31.4	-31.4	830	1.111	1.131
R—50EX10	0.692	31.4	0	830	1.210	1.230
R—50EX10	0.692	31.4	0	790	1.151	1.170
R—50EX20	0.692	62.8	0	590	1.060	1.074
R—50EX30	0.692	94.2	0	480	1.017	1.029
R—50EX11	0.692	31.4	31.4	730	1.230	1.248
R—50EX21	0.692	62.8	62.8	550	1.223	1.237
R—50EX21	0.692	62.8	62.8	525	1.167	1.181
R—50EX31	0.692	94.2	94.2	450	1.233	1.244
R—76EX2-1	1.033	62.8	-62.8	610	1.188	1.217
R—76EX1-1	1.033	31.4	-31.4	790	1.325	1.363
R—76EX10	1.033	31.4	0	700	1.270	1.304
R—76EX10	1.033	31.4	0	690	1.252	1.285
R—76EX20	1.033	62.8	0	560	1.231	1.259
R—76EX30	1.033	94.2	0	450	1.150	1.173
R—76EX11	1.033	31.4	31.4	590	1.224	1.253
R—76EX21	1.033	62.8	62.8	450	1.202	1.226
R—76EX31	1.033	94.2	94.2	380	1.227	1.248
R-100EX3-1	1.364	94.2	-94.2	450	1.244	1.274
R-100EX3-1	1.364	94.2	-94.2	465	1.286	1.317
R-100EX2-1	1.364	62.8	-62.8	601	1.499	1.538
R-100EX1-1	1.364	31.4	-31.4	705	1.554	1.599
R-100EX10	1.364	31.4	0	514	1.209	1.242
R-100EX20	1.364	62.8	0	439	1.214	1.243
R-100EX30	1.364	94.2	0	397	1.250	1.277
R-100EX30	1.364	94.2	0	384	1.209	1.235
R-100EX11	1.364	31.4	31.4	438	1.153	1.181
R-100EX21	1.364	62.8	62.8	362	1.184	1.209
R-100EX21	1.364	62.8	62.8	357	1.168	1.192
R-100EX31	1.364	94.2	94.2	327	1.263	1.287
R-100EX31	1.364	94.2	94.2	304	1.175	1.196
statistical evaluation			mean value		1.214	1.239
			standard deviation		0.110	0.117

Maximum compression at free longitudinal edge		
Stress distribution	Effective widths	Buckling factor k
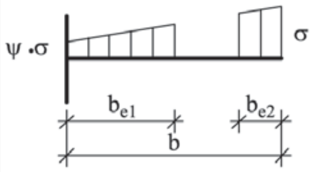	$1 \geq \psi \geq 0$ $\frac{b_{eff}}{b} = \rho$ $\frac{b_{e2}}{b} = \frac{0,226}{\bar{\lambda}_p^2}$	$1 \geq \psi \geq -2$ $k = \frac{1,7}{3+\psi}$
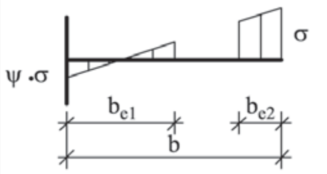	$0 \geq \psi \geq -1$ $\frac{b_{eff}}{b} = \left(\frac{\rho-\psi}{1-\psi}\right)$ $\frac{b_{e2}}{b} = \frac{0,226}{\bar{\lambda}_p^2}$	
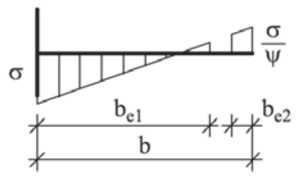	$\psi \leq -1$ $\frac{b_{eff}}{b} = \left(\frac{\rho-\psi}{1-\psi}\right)$ $\frac{b_{e2}}{b} = \frac{0,226}{\bar{\lambda}_p^2}\left(\frac{2}{1-\psi}\right)$	$-2 \geq \psi \geq -3$ $k = 3,3\,(1+\psi) + 1,25\,\psi^2$ $\psi \leq -3$ $k = \frac{(1-\psi)^2}{3,4}$
Maximum compression at supported longitudinal edge		
Stress distribution	Effective widths	Buckling factor k
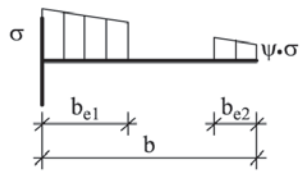	$1 \geq \psi \geq 0$ $\frac{b_{eff}}{b} = \rho$ $\frac{b_{e2}}{b} = \frac{0,226}{\bar{\lambda}_p^2}$	$1 \geq \psi \geq 0$ $k = \frac{1,7}{1+3\psi}$
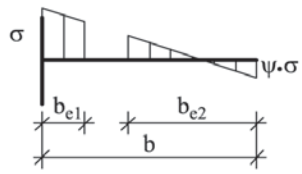	$0 \geq \psi \geq -1$ $\frac{b_{eff}}{b} = \left(\frac{\rho-\psi}{1-\psi}\right)$ $\frac{b_{e2}}{b} = \frac{0,226}{\bar{\lambda}_p^2} + \left(\frac{\psi}{\psi-1}\right)$	$0 \geq \psi \geq -1$ $k = 1,7 - 5\,\psi + 17,1\,\psi^2$
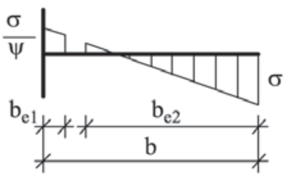	$\psi \leq -1$ $\frac{b_{eff}}{b} = \left(\frac{\rho-\psi}{1-\psi}\right)$ $\frac{b_{e2}}{b} = \frac{0,226}{\bar{\lambda}_p^2}\left(\frac{2}{1-\psi}\right) + \left(\frac{\psi}{\psi-1}\right)$	$\psi \leq -1$ $k = 5,98\,(1-\psi)^2$

Fig. 4 Effective widths for outstand compression elements loaded by bending and compression of their transverse edges